Effect of oxygen adsorption on the structure and spin-reorientation transition of Fe films on Cu(1 1 25)

Xucun Ma[a)]
State Key Laboratory for Surface Physics, Chinese Academy of Sciences, Beijing 100080, People's Republic of China and Max-Planck-Institut fuer Mikrostrukturphysik, Weinberg 2, D-06120 Halle/Saale, Germany

J. Barthel and M. Klaua
Max-Planck-Institut fuer Mikrostrukturphysik, Weinberg 2, D-06120 Halle/Saale, Germany

(Received 18 July 2003; accepted 8 December 2003)

The morphology, structure, and magnetism of Fe films on an oxygen-precovered, stepped Cu(1 1 25) surface are investigated by scanning tunneling microscopy, low-energy electron diffraction, and magneto-optical Kerr effect analysis. After exposure of Cu(1 1 25) to about 600 L of oxygen at 493 K, a well-ordered $(2\sqrt{2}\times\sqrt{2})$R45° superstructure is formed. The O-induced structure has a zig-zag morphology, showing a high density of facets and is very stable during subsequent Fe deposition. Fcc Fe can be stabilized up to 20 monolayer (ML) thickness, while the magnetization of the films reorients from perpendicular to in-plane at 15 ML. From 24 ML, the linear extrapolation line of the thickness dependence of the Kerr intensity of the transformed bcc Fe films does not go along with the pure fully magnetized bcc Fe films. We conclude that oxygen adsorption strongly affects the structure and spin-reorientation transition of Fe films. © *2004 American Institute of Physics.* [DOI: 10.1063/1.1644635]

I. INTRODUCTION

As a prototype system for the study of magnetic thin films, Fe epitaxially grown on Cu(001) has attracted considerable interest because of its structural richness and the unusual magnetic behavior.[1–10] A well-known magnetic and structural phase diagram of Fe films grown at room temperature shows that below 4 ML, the Fe film is tetragonally distorted (fct phase) with increasing perpendicular magnetization. At a thickness larger than about 4 ML and until 12 ML, the Fe film is fcc and then undergoes a fcc–bcc structural transformation, showing a decreasing perpendicular magnetization. At 12 ML, the spin-reorientation transition (SRT) from perpendicular to in-plane occurs, resulting from the martensitic fcc–bcc transformation of Fe films. Previous studies on this system have shown that a fcc–bcc structural transformation takes place before the SRT.

In fact, the critical thickness of structural and magnetic transitions of Fe films delicately depends on preparation conditions, such as growth temperature,[11] growth technique,[12] and surfactants.[13,14] Since surfactants generally exhibit a drastic effect on altering the balance of surface and interface free energies and strain that control epitaxial growth modes, this has provided us with the opportunity to manipulate magnetic properties of the films.[15,16] For example, the coadsorption of carbon- and oxygen-containing molecules $(CO,C_2H_2+O_2)$ has a strong effect on stabilizing γ-Fe films up to a 60 ML thickness.[13] H_2 adsorption of RT grown Fe films can change the magnetic properties and structure to be very similar to those observed for low-temperature-grown (100 K) Fe films.[14] It was noticed that oxygen adsorption can affect the growth of Fe films and their magnetization direction.[17,18] However, no comprehensive investigation has been performed to study the effect of the oxygen surfactant on the growth and magnetic properties of Fe grown on Cu(001).

In the present study, RT-grown Fe films on the oxygen-precovered, stepped Cu(1 1 25) substrate in the thickness regime of the fcc–bcc structural transformation are well-prepared by molecular-beam epitaxy method. Cu(1 1 25) substrate is chosen because from the preceding experiments,[19] it became evident that the degree of perfection of the oxygen-induced reconstruction of Cu(001) terraces which, in turn, is the prerequisite for layer-by-layer fcc Fe growth on Cu(001) is enhanced by the proximity of surface steps. Our scanning tunneling microscopy (STM) results demonstrated that a well-ordered $(2\sqrt{2}\times\sqrt{2})$R45° superstructure is formed after oxygen adsorption, which may play a role in the subsequent Fe growth. Here, the morphology and structure of the films are characterized by STM and low-energy electron diffraction (LEED), respectively. We use magneto-optical Kerr effect (MOKE) technique to measure the magnetic properties of such Fe films. Our investigations clearly demonstrate that oxygen strongly affects the thickness where the fcc–bcc phase transformation begins, while the SRT from perpendicular to in-plane easy axis of magnetization occurs at about 15 ML before the structural transformation starts at 20 ML.

II. EXPERIMENT

The experiments were carried out on a Cu(1 1 25) surface under UHV conditions (base pressure 2×10^{-11} mbar). The (1 1 25) surface is vicinal to (001), with a miscut angle

a)Electronic mail: xcma@aphy.iphy.ac.cn

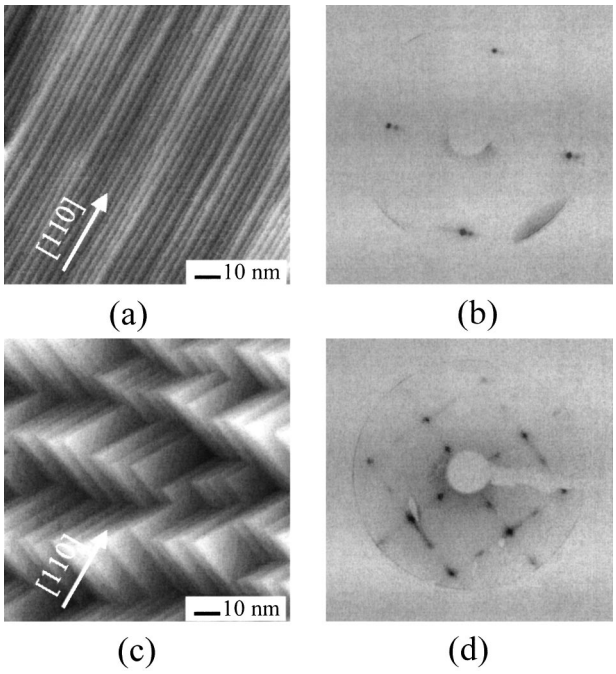

FIG. 1. (a) STM image of the clean Cu(1 1 25) surface showing monatomic steps parallel to [110]. (b) Corresponding LEED pattern at $E=50.4$ eV. (c) STM image of the Cu(1 1 25) surface after dosing with 600 L oxygen at 493 K showing the characteristic facetting structure with step edges running parallel to ⟨100⟩ or ⟨010⟩. (d) Image of the $(2\sqrt{2}\times\sqrt{2})$R45° LEED pattern obtained after oxygen deposition on Cu(1 1 25) at $E=45.5$ eV.

of 3.2°. The surface is characterized by flat (001) terraces in average 3.2 nm (=12.5 nearest-neighbor Cu-atom distances) wide, separated by monoatomic steps. The surface step edges run parallel to the [110] direction. The substrate was cleaned by several cycles of Ar^+ ion sputtering (1 keV) followed by annealing at 873 K. Both a sharp LEED $p(1\times1)$ pattern and an Auger spectrum, which did not show contaminants within the sensitivity limit, indicated high substrate quality. The surface morphology of the clean substrate was also examined by STM, a typical image of which is shown in Fig. 1(a). It shows steps parallel to the [110] direction as indicated by the arrow with a very narrow spread of terrace widths. Due to the regular step arrangement on the Cu(1 1 25) surface, each spot in the corresponding LEED pattern [Fig. 1(b)] is split into a doublet.

Oxygen exposure was carried out by using a dose valve. The chamber for the gas exposure has been pumped by a turbomolecular pump only, thus excluding oxygen ionization. In the following the amount of oxygen dosage is given in units of Langmuirs ($1\ \mathrm{L}=1\times10^{-6}$ Torr s). For Fe deposition onto the oxygen-dosed sample, which was kept near RT (295 K), we employed thermal evaporation of 99.999% purity Fe from a Knudsen cell. A stable evaporation rate of about 0.2 ML/min as controlled by a quartz monitor could be achieved. Two different kinds of samples were prepared: (i) series of films of *uniform* thickness for structure and morphology characterization and (ii) *wedge-shaped* films to study the thickness dependent magnetic properties. Within the wedges, the film thickness varies in five discrete steps of 2 ML along a sample diameter of 10 mm. The MOKE experiments were carried out at 130 K shortly after film deposition, comprising a cool-down time interval of about 1 h.

III. RESULTS AND DISCUSSION

A. Structure and morphology

After exposure of Cu(1 1 25) to about 600 L of oxygen at 493 K, a well-ordered $(2\sqrt{2}\times\sqrt{2})$R45° superstructure is formed. The morphology of the surface dosed with oxygen is shown in the STM image in Fig. 1(c). The surface is now characterized by a zig-zag pattern of ⟨100⟩-oriented step edges, while the [110]-oriented step edges of the clean surface have completely disappeared. Few (001) terraces have grown much wider (10 nm versus 3.2 nm), but the majority has become narrow due to step bunching. Figure 1(d) shows the two-domain $(2\sqrt{2}\times\sqrt{2})$R45° LEED pattern. Structure models of the (001) facet on the basis of STM, LEED, and x-ray diffraction analyses[20–23] on different systems suggest a missing row model along ⟨100⟩ directions, where 25% of the Cu sites are vacant, while along each missing Cu row to both sides stable Cu–O–Cu chains are formed. The Cu atoms squeezed out of the surface diffuse and give rise to a significant mass transport.

Structural changes of vicinal copper surfaces can be induced by oxygen adsorption resulting from oxygen organization along the steps and the destabilization of the step periodicity. Facetting of vicinal $(11n)$ surfaces upon oxygen exposure has been investigated thoroughly (with emphasis on $n<7$) in the past, as reviewed by Sotto[24] and by Besenbacher.[25] It was found that (104) and (014) facets, respectively, are the most stable surface configurations in the regime of oxygen saturation in the temperature range of 300 to 500 K. Again, linear Cu–O–Cu bonds along ⟨100⟩-oriented step edges stabilize this particular type of facets. In addition, a further row of adsorbed oxygen atoms is running parallel to the steps in the middle of each facet. The LEED pattern of {104} facets is identical to that of the two-domain $(2\sqrt{2}\times\sqrt{2})$R45° superstructure on (001) faces. In our case, the surface parts containing a high density of ⟨100⟩-oriented steps do not fully develop into stable (104) or (014) facets. The smallest observable step distance (~1 nm) is the one characteristic of {104} facets.

In general, the formation of the superstructure as well as of the facets is a thermally activated process and is related to the creation of stable Cu–O–Cu bond chains along ⟨110⟩ directions. The zig-zag-like surface morphology obtained immediately after oxygen exposure was found to be very stable in the course of further experiments, in particular during subsequent Fe deposition.

The structure and morphology of the Fe/O/Cu(1 1 25) surface is illustrated in Fig. 2. We will denote the growing film on the oxygen predosed substrate as Fe/O/Cu(1 1 25) although from Auger electron spectroscopy, it follows that oxygen floats to the surface of the film. Figure 2 displays STM and LEED images obtained on the Fe/O/Cu(1 1 25) system for different Fe thicknesses. Figures 2(a) and 2(c) show the surface morphology of 20 and 30 ML samples, respectively. These images can be considered as representative for the given thickness range, while for Fe thickness

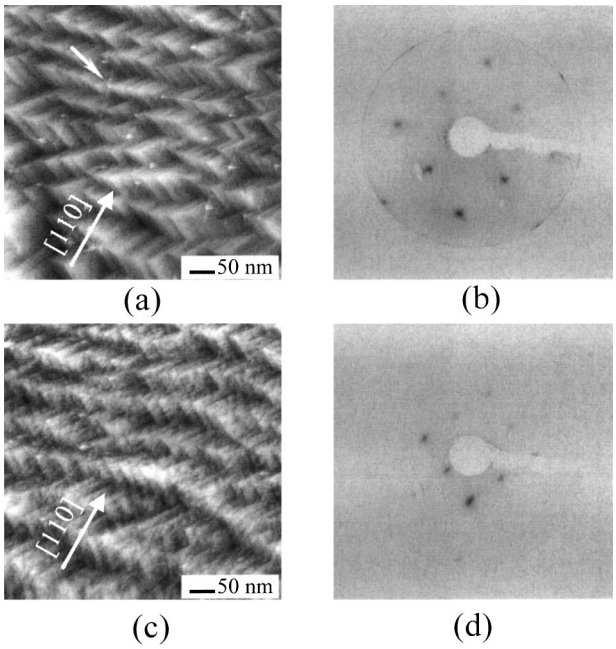

FIG. 2. (a) STM image after deposition of 20 ML on the O/Cu(1 1 25) surface. The facet structure characteristic for the O/Cu(1 1 25) surface is still maintained, the bright, needle-shaped structures (see arrow) are interpreted as bcc-Fe nucleation centers. (b) $c(2\times2)$ LEED pattern of the 20 ML film at $E=66.5$ eV. (c) STM image after deposition of 30 ML Fe. The bright, stripe-shaped structures are dominant in the image. (d) LEED pattern of a 25 ML film taken at $E=127.0$ eV.

below 20 ML, the STM images closely resemble those obtained for the O/Cu(1 1 25) surface prior to Fe deposition, as shown in Fig. 1(c). As can be seen in Fig. 2(a) at an Fe coverage of about 20 ML, the STM image reveals the formation of a few narrow, elongated features, one example being indicated by the arrow. In general, these bright, needle-like structures in the STM image are well known as fingerprints of bcc Fe precipitates in the Fe/Cu(001) system.[2,26] The long axis of these bcc precipitates is oriented either along the [110] or the [−110] direction. The precipitates are crossing a large number of surface steps without noticeable interaction. Many more of these needle-like features are observed at 30 ML, where they cover most of the surface. The gradual morphology change evidenced by the comparison between the 20 and 30 ML samples suggests that the Fe film surface undergoes a continuous fcc–bcc transformation from 20 ML on.

The LEED patterns displayed in Figs. 2(b) and 2(d) were taken at an Fe coverage of 20 ML (electron energy 66.5 eV) and 25 ML (127 eV), respectively. In general, we observe a $c(2\times2)$ LEED pattern in the coverage range between 7 and 25 ML. This $c(2\times2)$ superstructure can be interpreted by a model in which, during Fe deposition, the O atoms float on the surface. In this way the O atoms promote layer-by-layer growth by forcing the Fe atoms to stay on fcc lattice sites rather than to crystallize in a bcc Fe-like structure. The $c(2\times2)$ reconstruction on a quite smooth and ordered film surface below 25 ML is self-reproducing during growth. However, with increasing Fe film thickness the LEED pattern becomes observable at higher beam energies only. The gradual change of the LEED patterns above 25 ML gives evidence for our conclusion that the fcc–bcc transformation process is proceeding, followed by increasing bcc-needle density and surface roughness.

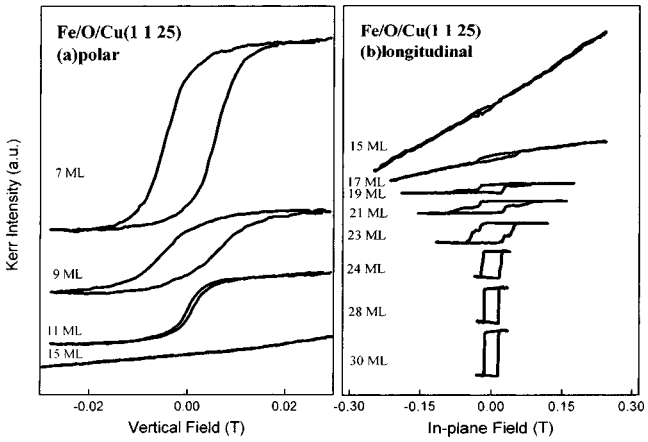

FIG. 3. Kerr loops for Fe/O/Cu(1 1 25) recorded at 130 K in polar (left) and longitudinal (right) geometry.

B. Magnetic properties

The magnetic properties were studied using *in situ* MOKE in longitudinal and polar geometry in order to identify the easy axis of magnetization and to measure the evolution of the saturation Kerr signal (ellipticity) with film thickness.

Thickness-dependent Kerr measurements for Fe/O/Cu(1 1 25) were carried out in the coverage range between 7 and 30 ML. The polar and longitudinal hysteresis loops recorded at 130 K sample temperature are shown in Figs. 3(a) and 3(b), respectively. Note that all loops displayed in Fig. 3(b) are recorded with external field applied along the [110] direction. In the region between 7 and 11 ML, the films exhibit a perpendicular easy axis; however, the Kerr signal decreases with increasing thickness. This is representative of fcc Fe films showing the perpendicular magnetization as compared to bcc Fe films with the in-plane magnetization. At 15 ML, the polar signal cannot be detected; instead, a small longitudinal signal is observed. At higher Fe thickness, the longitudinal hysteresis loops show a gradual change in shape and a slow rise in magnitude with increasing thickness. Between 21 and 24 ML, the Kerr signal rises steeply with coverage ending up in a regime of linear growth with film thickness after 24 ML (see Fig. 4). From this observation, we conclude that the SRT from perpendicular to in-plane takes place at the thickness of about 15 ML.

Figure 4 gives a comprehensive overview of thickness-dependent structural and magnetic properties of Fe films on oxygen-precovered Cu(1 1 25) substrate. With regard to the structural properties of the Fe/O/Cu system, due to oxygen adsorption on the Cu(1 1 25) surface, the formation of $c(2\times2)$ superstructure during Fe growth provides a better layer-by-layer film growth. Fcc Fe films can be stabilized up to 20 ML. Even at 30 ML, apart from a high density of bcc-needle structure presented on the surface, the main morphology still resembles that at 20 ML.

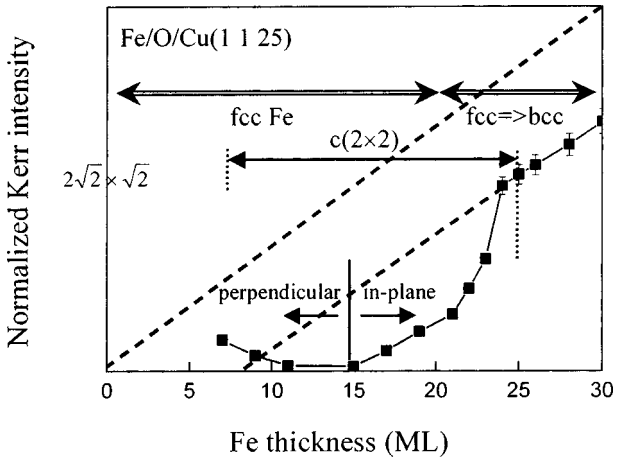

FIG. 4. Schematic illustration of structural and magnetic evolution of Fe films on oxygen-adsorbed Cu(1 1 25) substrate. Structural and SR transitions are indicated.

With respect to magnetic properties of the Fe/O/Cu system, although the nucleation of first bcc precipitates is observed only at about 20 ML, from where, on the whole, structural transition extends over a thickness range of at least 10 ML, SRT takes place already at about 15 ML. This finding is in contrast with many other studies on the Fe/Cu(001) system. Distinct structural differences exist between them, but critical thickness of SRT has a shift towards an about 3 ML larger value only than that in the Fe/Cu(001) system. Therefore, an interesting question arises: How can we understand the big deviation of critical thickness between structural and spin-reorientation transitions in such a system? In the following we give possible explanations.

In practice, for the Fe/Cu(001) system, even though the structural transition itself could closely lead to a SRT, up to now, no direct information can be given that the structural transition is prerequisite for the SRT. This is because the origin of the SR is the usual balance between the surface and shape anisotropy, rather than the formation of bcc structure. Previous studies have shown that the fct phase and the bcc phase are formed in the films below 4 ML and above 12 ML in the Fe/Cu system, respectively, while a phase consisting of antiferromagnetic (AF) fcc Fe covered with ferromagnetic (FM) fct Fe surface layers can be realized between 4 and 12 ML. Moreover, a positive surface anisotropy, as in the case of thin Fe films on Cu, leads to an easy axis of magnetization perpendicular to the film before completely transforming to bcc Fe phase. In our case, the graduate decrease of the normalized Kerr intensity in the 7–11 ML thickness range with an easy axis of magnetization perpendicular to the film is observed, which is similar to that in the 4–12 ML thickness range of the Fe/Cu system. It is possible that a phase consisting of AF and live layers also presents in the studied system. Based on our current experiment, we cannot give further evidence to confirm this. If the graduate decrease is indeed caused by the graduate change of the FM phase to the AF phase of the fcc Fe film, the relative portion of the surface anisotropy (proportional the surface area) to the shape anisotropy (proportional to the FM volume) should change accordingly. However, the use of the stepped substrate and the effect of oxygen adsorption on the stepped substrate do respond to the complex competition mechanism among the anisotropies in our unusual structures, resulting in the SR of the Fe/O/Cu system in the end.

Step-induced anisotropy has been investigated in recent years on the study of the magnetism of ultrathin films.[27–30] The film on the stepped substrate exhibits an in-plane, uniaxial magnetic anisotropy with the easy magnetization axis perpendicular[27] or parallel[28,30] to the step edges, depending on the detailed physical systems. In the Fe films grown on the stepped Ag(001) substrate (6° vicinal angle), Kawakami *et al.* found a SRT shift to an ~10% larger critical thickness due to the step-induced anisotropy contribution. The strength of this anisotropy varies quadratically with step density.[30] The Cu(1 1 25) surface has a reduced symmetry with respect to the Cu(001) surface. Easy axis parallel to the [110] steps has been found on Cu(1 1 n) substrates when growing ultrathin Co films.[29] Compared to Ref. 30, the Cu(1 1 25) surface has a lower step density with a smaller vicinal angle (3.2°). Thus, a much smaller step-induced anisotropy can be speculated. Since the SRT in the Fe/Cu(001) system takes place at 12 ML, SRT in Fe/Cu(1 1 25) system may occur at about 12.6 ML, at most showing a little shift of about 0.6 ML larger than that in the Fe/Cu(001) system. Therefore, step-induced anisotropy might not the major reason for the large deviation of critical thickness between structural and SR. It is worth noting that no similar studies with respect to the influence of surface steps on in-plane anisotropy have been carried out so far for fcc Fe on vicinal Cu(001) because this system under conventional growth conditions (thermal evaporation onto the clean substrate) is characterized by perpendicular uniaxial anisotropy.

The effect of oxygen adsorption induced structural changes has been elucidated by STM and LEED analyses. The oxygen-dosed Cu(1 1 25) surface is characterized by [100] and [010] steps. From the shape changes of the loops along the [110] direction, we can give such a proposition: As long as this orientation prevails, the fcc Fe film displays a fourfold magnetic anisotropy with easy axis of magnetization along the surface step directions. At an Fe coverage>24 ML, where the surface contains a noticeable amount of bcc precipitates, the films start to display uniaxial magnetic in-plane anisotropy along [110], the initial surface step direction, which is in agreement with the earlier discussion that uniaxial magnetic anisotropy occurs in low-symmetry surfaces. The magnetism of Fe films influenced by oxygen surfactant indicates that surface anisotropy is sensitive to the coverage of oxygen on the Fe/vacuum interface.[31,32] The study of Pappas *et al.*[18] on Fe/Cu(001) has given direct evidence, that oxygen induces a switching of the easy axis from perpendicular to in-plane at low dosages (<1 L) introduced after film growth. In that context the presence of oxygen is likely to reduce the magnitude of the surface anisotropy or even to change its sign to flip the easy axis into the film plane. The study of Peterka *et al.* further confirms that the reorientation of magnetization results from the adsorbate-induced change in the magnetic interface anisotropy energy of the Fe/vacuum interface. For our system Fe/O/Cu(1 1 25) it seems plausible that on the one hand the delayed fcc–bcc

transformation; that is, the persistence of an fcc Fe/vacuum interface would support a positive surface anisotropy, while, on the other hand, the presence of oxygen tends to reduce surface anisotropy or even switch it to the negative side. Therefore, this probably causes an SRT shift towards a lower thickness with respect to that without oxygen adsorption. The similar situation has been reported for the Fe/Cu(001) system with hydrogen adsorption.[14] Combined with all kinds of anisotropy contributions in our system, the effects in sum then maintain the SRT critical thickness at about 15 ML.

The total magnetic moment (Kerr ellipticity, respectively) versus film thickness curve for the Fe/O/Cu(1 1 25) system (Fig. 4) can be divided into four parts. The first region ranges from 7 to 15 ML, where the SRT occurs. The polar Kerr signal in this region decreases with increasing thickness vanishing around the transition point. The second region extends from 15 to 21 ML with a slow recovery of the Kerr signal (now in the film plane). Polar and in-plane saturation values are scaled according to the intrinsic calibration of our MOKE system to display the same height for identical saturation magnetic moment, measured in either easy or hard directions. The films in this coverage regime have pure fcc structure (below 20 ML). The third region extends from 21 to 24 ML and is characterized by a steep increase of the Kerr signal.

Above about 24 ML, the Kerr signal linearly increases with thickness, which we assign as the fourth region. Using the bulk Fe magnetic moment of 2.2 μ_B per atom for the bcc phase, the reference curve for the in-plane Kerr signal of a fully FM magnetized bcc Fe film as function of film thickness can be drawn for comparison (the dashed line in Fig. 4). This curve is based on the internal calibration of our MOKE system carried out on bcc Fe/Cu(001) films above 12 ML thickness, extrapolated back to 0 ML film thickness. Comparing the dashed line and our present curve for the Fe/O/Cu(1 1 25) system in the interval from 24 to 30 ML one finds that both lines are parallel to each other, but with a constant offset between them. This implies that the films in this range do not only consist of purely bcc Fe layers of full 2.2 μ_B moment per atom. The constant offset suggests that the structure may be composed of a surface FM phase and an underlying nonmagnetic (NM) or AF phase. The number of NM layers can be obtained by extrapolating the curve to the abscissa, the intersection is at about 8 ML. This magnetic structure model is in agreement with the structural properties of the films in the coverage region between 24 and 30 ML. As discussed before, no LEED pattern characteristic for bcc Fe can be observed, even up to 30 ML. The films maintain fcc structure in the bulk as below 20 ML and a $c(2\times2)$ reconstruction on large parts of their surface. Possibly, the nucleating FM surface bcc Fe phase stimulates the underlying fcc Fe layers to switch into a FM phase from 20 ML on. This effect penetrates an increasing depth zone except the eight lowest fcc Fe layers.

IV. SUMMARY

In summary, we have used LEED, STM, and MOKE to study the structural and magnetic properties of the Fe films deposited at RT on oxygen-adsorbed Cu(1 1 25) surface with about 600 L of oxygen at 430 K, showing a $(2\sqrt{2}\times\sqrt{2})$R45° superstructure.

A distinct difference in the structural evolution is observed in the Fe/O/Cu system. The fcc–bcc transition is largely inhibited until the nucleation of first bcc surface precipitates at about 20 ML. This is interpreted as due to the presence of oxygen as surfactant. The Fe films on the oxygen-adsorbed Cu(1 1 25) substrate show a $c(2\times2)$ superstructure up to 25 ML. The spin reorientation from perpendicular to in-plane occurs at a thickness of about 15 ML. The effects of step- and oxygen-adsorption-induced anisotropy are discussed. Within the coverage region between 20 and 30 ML, we observe a steeply increasing magnetic moment of the film, while the linear extrapolation line of the thickness dependence of the Kerr intensity of the transformed bcc Fe films does not go along with the pure, fully magnetized bcc Fe films. This may mean that the films above 24 ML are structurally composed of a thin bcc Fe surface phase on the top, and constantly of a few layers of NM or AF fcc Fe underneath.

ACKNOWLEDGMENTS

One of the authors (X. Ma) thanks the support from MPI Halle during the stay in Halle, Dr. H. L. Meyerheim and Prof. J. Kirschner for helpful discussions, and Mr. G. Kroder for technical support.

[1] J. Thomassen, F. May, B. Feldmann, M. Wuttig, and H. Ibach, Phys. Rev. Lett. **69**, 3831 (1992).
[2] M. Wuttig, B. Feldmann, J. Thomassen, F. May, H. Zillgen, A. Brodde, H. Hannemann, and H. Neddermeyer, Surf. Sci. **291**, 14 (1993).
[3] P. Bayer, S. Müller, P. Schmailzl, and K. Heinz, Phys. Rev. B **48**, 17611 (1993).
[4] T. Krafe, P. M. Marcus, and M. Scheffler, Phys. Rev. B **49**, 11511 (1994).
[5] D. Li, M. Freitag, J. Pearson, Z. Q. Qiu, and S. D. Bader, Phys. Rev. Lett. **72**, 3112 (1994).
[6] J. Giergiel, J. Kirschner, J. Landgraf, J. Shen, and J. Woltersdorf, Surf. Sci. **310**, 1 (1994).
[7] R. D. Ellerbrock, A. Fuest, A. Schatz, W. Keune, and R. A. Brand, Phys. Rev. Lett. **74**, 3053 (1995).
[8] S. Müller, P. Bayer, C. Reischl, K. Heinz, B. Feldmann, H. Zillgen, and M. Wuttig, Phys. Rev. Lett. **74**, 765 (1995).
[9] J. Shen, Ch. V. Mohan, P. Ohresser, M. Klaua, and J. Kirschner, Phys. Rev. B **57**, 13674 (1998).
[10] R. E. Camley and D. Li, Phys. Rev. Lett. **84**, 4709 (2000).
[11] H. Zillgen, B. Feldmann, and M. Wuttig, Surf. Sci. **321**, 32 (1994).
[12] H. Jenniches, J. Shen, Ch. V. Mohan, S. Sundar Manoharan, J. Barthel, P. Ohresser, M. Klaua, and J. Kirschner, Phys. Rev. B **59**, 1196 (1999).
[13] A. Kirilyuk, J. Giergiel, J. Shen, M. Straub, and J. Kirschner, Phys. Rev. B **54**, 1050 (1996).
[14] R. Vollmer and J. Kirschner, Phys. Rev. B **61**, 4146 (2000).
[15] C. Tölkes, R. Struck, R. David, P. Zeppenfeld, and G. Comsa, Phys. Rev. Lett. **80**, 2877 (1998).
[16] W. L. Ling, Z. Q. Qiu, O. Takeuchi, D. F. Ogletree, and M. Salmeron, Phys. Rev. B **63**, 024408 (2001).
[17] W. F. Egelhoff, Jr. and D. A. Steigerwald, J. Vac. Sci. Technol. A **7**, 2167 (1989).
[18] D. P. Pappas, K.-P. Kamper, B. P. Miller, H. Hopster, D. E. Fowler, A. C. Luntz, C. R. Brundle, and Z.-X. Shen, J. Appl. Phys. **69**, 5209 (1991).
[19] A. Kida (unpublished).
[20] H. C. Zeng, R. A. McFarlane, and K. A. R. Mitchell, Surf. Sci. **208**, L7 (1989).
[21] F. Jensen, F. Besenbacher, E. Lægsgaard, and I. Stensgaard, Phys. Rev. B **42**, 9206 (1990).

[22] I. K. Robinson, E. Vlieg, and S. Ferrer, Phys. Rev. B **42**, 6954 (1990).
[23] D. A. Walko and I. K. Robinson, Surf. Rev. Lett. **6**, 851 (1999).
[24] M. Sotto, Surf. Sci. **260**, 235 (1992).
[25] F. Besenbacher and J. K. Norskov, Prog. Surf. Sci. **44**, 5 (1993).
[26] K. Kalki, D. D. Chambliss, K. E. Johnson, R. J. Wilson, and S. Chiang, Phys. Rev. B **48**, 18344 (1993).
[27] J. Chen and J. L. Erskine, Phys. Rev. Lett. **68**, 1212 (1992).
[28] A. Berger, U. Linke, and H. P. Oepen, Phys. Rev. Lett. **68**, 839 (1992).
[29] D. S. Chuang, C. A. Ballentine, and R. C. O'Handley, Phys. Rev. B **49**, 15084 (1994).
[30] R. K. Kawakami, Ernesto J. Escorcia-Aparicio, and Z. Q. Qiu, Phys. Rev. Lett. **77**, 2570 (1996).
[31] B. Heinrich, J. F. Cochran, A. S. Arrot, S. T. Purcell, K. B. Urquhart, J. R. Dutcher, and W. F. Egelhoff, Appl. Phys. A: Solids Surf. **49**, 473 (1989).
[32] D. Peterka, A. Enders, G. Haas, and K. Kern, Phys. Rev. B **66**, 104411 (2002).